PROCEEDINGS OF SCIENCE

Search for the rare $K_S^0 \to \mu^+\mu^-$ decay

Giacomo Graziani*
on behalf of the LHCb collaboration
INFN Sezione di Firenze
E-mail: graziani@fi.infn.it

A search for the decay $K_S^0 \to \mu^+\mu^-$ is performed, based on a data sample corresponding to an integrated luminosity of 1.0 fb^{-1} of pp collisions at $\sqrt{s} = 7$ TeV collected by the LHCb experiment at the Large Hadron Collider. The observed number of candidates is consistent with the background–only hypothesis, yielding an upper limit of $\mathcal{B}(K_S^0 \to \mu^+\mu^-) < 11(9) \times 10^{-9}$ at 95 (90) % confidence level. This limit is below the previous measurement by more than a factor of thirty.

2013 Kaon Physics International Conference,
29 April-1 May 2013
University of Michigan, Ann Arbor, Michigan - USA

*Speaker.

PoS(KAON13)020

1. Introduction

The flavour–changing neutral–current (FCNC) decay mode $K^0 \to \mu^+\mu^-$ is probably the best illustration of how a search for a rare decay can give insight to "new" physics. Its suppression was one of the inputs leading to the prediction of the charm quark through the GIM mechanism before the discovery of the J/ψ meson. Possible intermediate states can give different contributions to the K^0_S and K^0_L modes. In the absence of CP violation, the K^0_L (K^0_S) mode could proceed only through S (P) wave. Before LHCb, the most sensitive search for the K^0_S mode was performed at the CERN PS in the early 70s, motivated by the possible enhancement of this mode through a relatively large CP violating effect. No events were observed, yielding an upper limit [1] $\mathscr{B}(K^0_S \to \mu^+\mu^-) < 3.1\times10^{-7}$ at 90 % confidence level. Current Standard Model (SM) calculations predict both K^0_L and K^0_S modes to be dominated by long distance contributions that are well constrained from the measurements of $\gamma\gamma$ modes. For the $K^0_L \to \mu^+\mu^-$ mode, a value of $(6.85\pm0.32)\times10^{-9}$ is expected [2], in excellent agreement with the experimental world average [3] $\mathscr{B}(K^0_L \to \mu^+\mu^-) = (6.84\pm0.11)\times10^{-9}$. For the K^0_S mode, the branching fraction is expected [4, 5] to be $(5.0\pm1.5)\times10^{-12}$, five order of magnitudes below the experimental limit cited above. Contributions from physics beyond the SM, notably via possible new light scalars, can affect the K^0_S mode exclusively. Enhancements up to one order of magnitude above the SM level would be well compatible with the present bounds from other $\Delta S = 1$ FCNC processes [5].

2. Kaons in LHCb

The LHCb experiment is conceived for the study of CP violation and rare decays in the heavy quark sector at the LHC. The detector [6] is thus optimized for the decays of b and c hadrons. However, the LHC is also a kaon factory, with about 10^{13} K^0_S produced within the LHCb acceptance per fb^{-1} of integrated luminosity. Moreover, about 40 % of those kaons decay within the length of the LHCb vertex locator (VELO). For such decays, the excellent vertexing and tracking capabilities of the detector allow to reconstruct the invariant mass of $K^0_S \to \pi^+\pi^-$ decays with a resolution of about 4 MeV/c^2. The other distinctive feature of the LHCb detector, the particle identification capabilities, can be exploited to identify the muons from the pions. A muon identification (μID) algorithm [7] determines if the detected tracks are compatible with hits in the downstream muon detector, also using the information from the calorimeters and the two RICH detectors of the experiment. The fraction of pions misidentified as muons is about 1%, for a muon identification efficiency of 97%, and is dominated by $\pi \to \mu\nu$ decays inside the detector.

The analysis is performed using the data collected during 2011, corresponding to an integrated luminosity of 1.0 fb^{-1}. The need for tight trigger requirements in the LHC environment turns out to be the most limiting experimental factor for this search. The LHCb hardware trigger level selects muons, using only hits from the muon detector, with transverse momentum (p_T) larger than 1.5 GeV/c, a relatively low threshold for b decays that results, on the contrary, in a low efficiency ($\sim$ 1 %) for $K^0_S \to \mu^+\mu^-$ decays. The other trigger level, the software–based high–level trigger, confirms the high–p_T muon candidate track from a full event reconstruction, and requires that is detached from the primary vertex. However, due to its limited output bandwidth, a prescale factor of two had to be applied. The events selected by these requirements constitute one of the

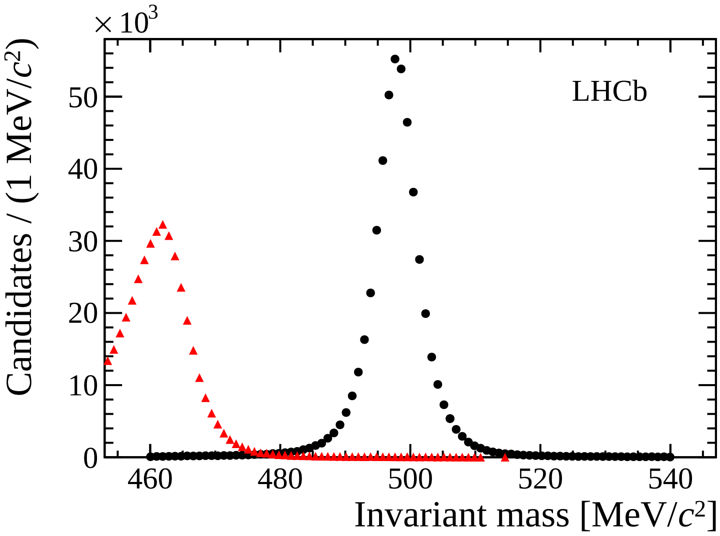

Figure 1: The invariant mass distribution for $K_S^0 \to \pi^+\pi^-$ candidates decaying inside the VELO is shown by black circles. The curve made of red triangles, obtained from the same events assigning the muon mass to the two decay products, represents the expected distribution for the events misreconstructed as $K_S^0 \to \mu^+\mu^-$.

two samples used for this analysis, called TOS (Trigger On Signal) in the following. The other sample is obtained by events triggered by particles other than the K_S^0 products (TIS sample, Trigger Independent of Signal). Due to the low trigger efficiency of the TOS sample, the inclusion of the TIS sample results in a non–negligible increase of the statistical sensitivity. Moreover, due to the absence of trigger biases, this second sample provides a valuable cross-check for systematic effects. The small fraction of events entering both categories, ~ 0.1 % of TOS events, are considered only in the TIS sample.

3. Search strategy

Candidates for the $K_S^0 \to \mu^+\mu^-$ decay are obtained from tracks with opposite charge identified as muons, forming a vertex with invariant mass compatible with the known K_S^0 mass value. Due to its abundance, similar topology and well known branching fraction, the $K_S^0 \to \pi^+\pi^-$ decay is the ideal normalization mode. It also constitutes the largest source of background, when both pions are misidentified as muons. In such case, the invariant mass of the kaon candidate is underestimated on average by ~ 40 MeV, corresponding to ten times the invariant mass resolution for decays within the VELO acceptance. By using only such decays, only the far tail of the $K_S^0 \to \pi^+\pi^-$ distribution is expected to contribute to the signal region, as illustrated in Fig. 1. The normalization sample for the TOS selection is obtained from randomly triggered events, as discussed later in Section 5, while for the TIS case the same trigger selection of the signal is used.

The same selection cuts, including requirements on the reconstruction quality and on kinematical variables, are applied to the signal and normalization modes, except for the μID criteria. Data–driven methods are used as much as possible to determine the backgrounds and efficiencies, while simulated events are mainly used for the validation of the analysis procedure. In particular, candidate events are counted in the signal region, defined as the invariant mass window from 492

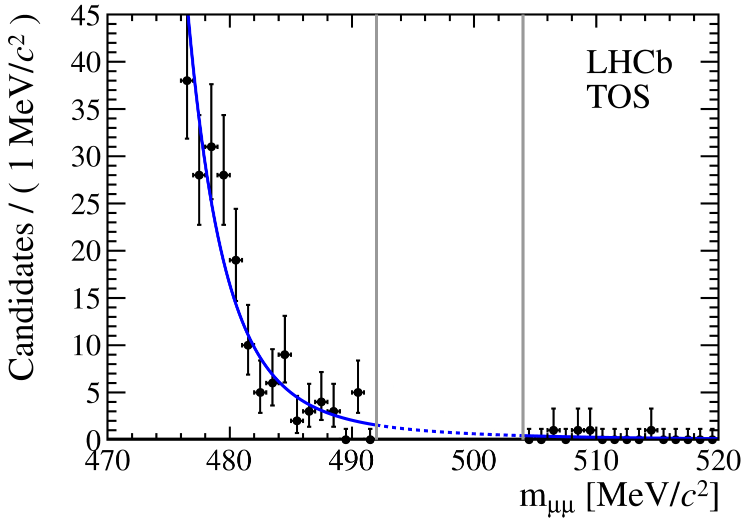

Figure 2: Invariant mass distribution in the sidebands region for all BDT bins of the TOS sample. Events in the signal region, kept blind during the development of the analysis, are not showed. The curve illustrates the fit used to predict the background yields expected in the signal region.

to 504 MeV/c^2, without using the shape of the distribution within the window, that can only be predicted using simulation for the $\mu^+\mu^-$ mode.

A multivariate classifier based on a Boosted Decision Tree (BDT) is developed to reduce the combinatorial background. The input variables, including kinematical and reconstruction quality variables as the decay length, the impact parameter and the χ^2 of the vertex fit, are carefully chosen in order to not distinguish the $\mu^+\mu^-$ and $\pi^+\pi^-$ modes, thus excluding the invariant mass and the μID–related variables. This allowed to use the $K^0_S \to \pi^+\pi^-$ mode to train the BDT for the signal, while the background was modeled using events in sidebands of the invariant mass distribution. An important discriminating variable turns out to be the position of the decay vertex, since sideband data show a relevant fraction of events located inside the VELO sensors, revealing a contribution from interactions with the detector material. Two different classifiers are optimized separately for the TOS and TIS samples. To avoid overtraining, the two BDTs are also trained separately for each half of the data sample, and applied to the other half. The analysis is performed in ten bins of the BDT output, after applying only a loose cut on it.

4. Backgrounds

The number of background events in each BDT bin is predicted using a fit to the mass sidebands, as illustrated in Fig. 2. The fit function consists of the sum of an exponential term modeling the combinatorial background, and an empirical function describing the tail of the $K^0_S \to \pi^+\pi^-$ contribution, validated on simulation. Possible sources of background peaking in the signal region are carefully considered, notably $K_{\mu 3}$ decays with a misidentified pion and low–momentum neutrino, $K^0 \to \mu^+\mu^-\gamma$ and $K^0_L \to \mu^+\mu^-$ decays. Using their known branching fractions and their detection efficiency from simulation, all of them are found to produce negligible event yields.

5. Normalization and efficiencies

The branching fraction for the $K^0_S \to \mu^+\mu^-$ decay is measured relatively to the normalization mode:

$$\frac{\mathscr{B}(K^0_S \to \mu^+\mu^-)}{\mathscr{B}(K^0_S \to \pi^+\pi^-)} = \frac{\varepsilon^{SEL}_{\pi\pi}}{\varepsilon^{SEL}_{\mu\mu}} \frac{1}{\varepsilon^{PID}_{\mu\mu}} \frac{\varepsilon^{TRIG}_{\pi\pi}}{\varepsilon^{TRIG}_{\mu\mu}} \frac{N_{K^0_S\to\mu^+\mu^-}}{N_{K^0_S\to\pi^+\pi^-}}, \tag{5.1}$$

where the efficiency ratio for the two modes is factorized for convenience in three terms:

- the ratio of selection and reconstruction efficiencies ε^{SEL}, that is the only factor obtained from simulation. The largest effect not canceling in the ratio comes from the interactions in the detector material that are more likely for pions than for muons. Since this effect is strongly momentum dependent, the simulated samples are reweighted to reproduce the rapidity and p_T distributions observed in $K^0_S \to \pi^+\pi^-$ data. The efficiency ratio is computed in kinematic bins and its value ranges from 0.6 to 0.85;

- the efficiency of the muon identification, only applied to the signal mode, is measured from real data, in bins of momentum p and p_T, using a "tag–and–probe" method on a clean sample of $J/\psi \to \mu^+\mu^-$ from b decays. This calibration sample is selected requiring the J/ψ vertex to be detached from the primary vertex, the invariant mass of the two tracks to be compatible with the known J/ψ mass, and the identification of one of the two muons. The trigger also relies solely on this "tag" muon. The other muon, not biasing the trigger and the selection at any level, is used to probe the muon identification procedure. The value ranges from 68 to 82 %, depending on the trigger sample and the BDT bin;

- the ratio of trigger efficiencies for reconstructed and selected events. For the TIS sample, the ratio is expected to equal unity since the trigger does not rely on the candidate K^0_S tracks; this is confirmed by simulation. The same event sample can be used to measure the event yields $N_{K^0_S\to\mu^+\mu^-}$ and $N_{K^0_S\to\pi^+\pi^-}$ from the selection with and without the μID requirements. For the TOS sample, where the muon identification is required at the trigger level, the use of a different trigger selection for the normalization mode is needed. Fully unbiased random triggers are used, so that $\varepsilon^{TRIG}_{\pi\pi}$ is simply the inverse of the prescale factor used for this trigger line, namely the fraction of pp collisions that are randomly selected. An absolute measurement of $\varepsilon^{TRIG}_{\mu\mu}$ is then needed. It is obtained using a sample of $B^+ \to J/\psi\ (\mu^+\mu^-)K^+$ decays that are not biased by the trigger. This is achieved by requiring that events are triggered by particles in the event other than the J/ψ and the kaon. The muon p and p_T spectra of such sample are reweighted to match those of the signal. For events passing the offline selection, notably requiring $p_T > 1.3$ GeV/c, $\varepsilon^{TRIG}_{\mu\mu}$ is found to be about 20%.

6. Systematic uncertainties

One of the main systematic uncertainty is related to the use of simulation to evaluate $\varepsilon^{SEL}_{\pi\pi}/\varepsilon^{SEL}_{\mu\mu}$, notably because of the uncertainty on the K^0_S production spectrum. Different reweighting schemes are compared, resulting in a relative uncertainty of about 20%. For the TOS sample the largest uncertainty comes from the knowledge of the efficiency of the random trigger, determined to be

PoS(KAON13)020

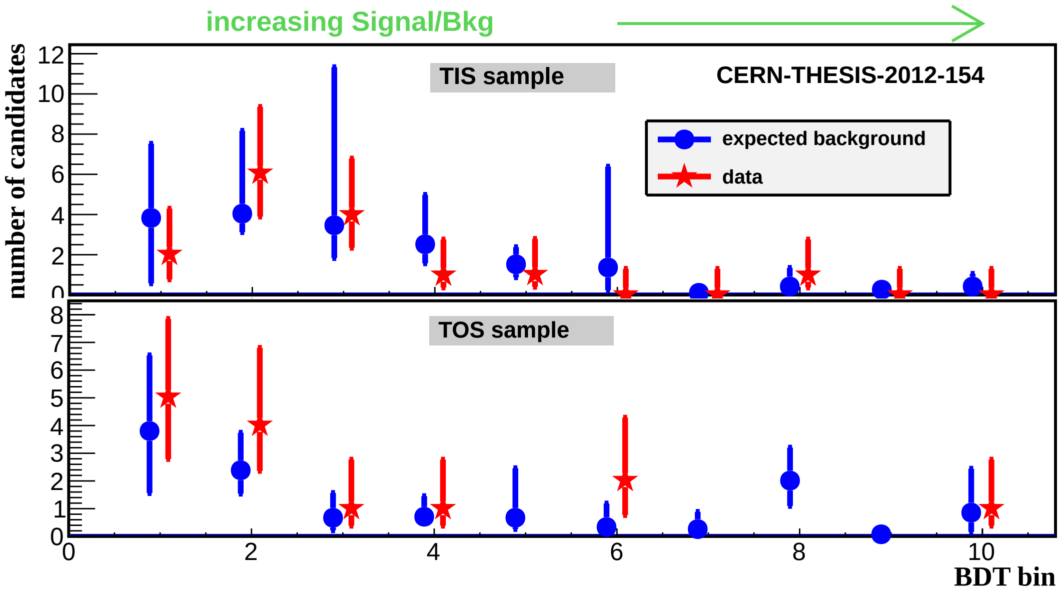

Figure 3: The event counts (red stars) observed in each BDT bin, separately for the TIS and TOS samples, are compared with the expectations from background (blue circles) [8].

$(2.70 \pm 0.76) \times 10^{-6}$. The large uncertainty is due to the fact that the prescale factor was not fixed, but dynamically changed to provide a constant rate for this unbiased trigger line. The data–driven methods used to estimate the μID and TOS trigger efficiencies were validated using simulation, the difference between the two evaluations being assigned as systematic uncertainty. The assumption of equal trigger efficiency for the signal and normalization modes in the TIS sample is also verified using simulation, with the statistical accuracy of such validation taken as systematic uncertainty. The uncertainty on $\mathscr{B}(K_S^0 \to \pi^+\pi^-)$ is also taken into account.

7. Results

Following a blind approach, events in the signal region were counted only after freezing the analysis procedure. The observed event counts in each BDT bin are compared with the background–only expectation in Fig. 3. No visible excess is found, and the BDT distribution of the few candidates follows the pattern predicted for the background, with only 2 events in the four most discriminating BDT bins. The observed yields are converted into an upper limit using the CLs method [9]. The result is shown in Fig. 4. The combination of the analysis of TOS and TIS samples brings [10]

$$\mathscr{B}(K_S^0 \to \mu^+\mu^-) < 11(9) \times 10^{-9}$$

at 95 (90) % confidence level.

8. Conclusions and Prospects

In conclusion, LHCb proved to be able to contribute to the physics of rare kaon decays, improving by a factor 34 the world's best limit on $K_S^0 \to \mu^+\mu^-$, dating back from 40 years ago. The

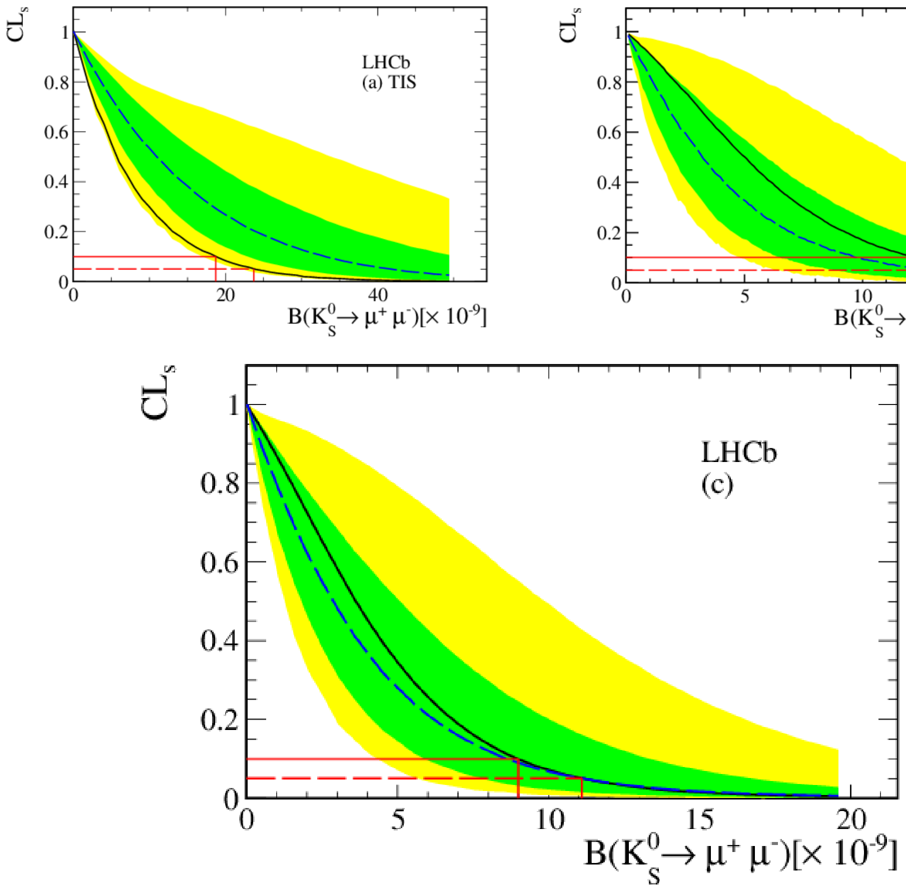

Figure 4: Upper limit on $\mathscr{B}(K^0_S \to \mu^+\mu^-)$ obtained using the CLs method from a) the TIS sample, b) the TOS sample, c) the combination of the two samples. For each value of the branching fraction, the curves show the CLs value, corresponding to an upper limit with confidence level 1−CLs. The dashed lines correspond to the median of the CLs distribution expected from simulated background–only experiments. The green (dark) and yellow(light) areas cover 68% and 95% of the distribution, respectively. The solid lines show the observed values from which the upper limits at 90% and 95% confidence level are obtained.

improved limit is still above the SM expectation by more than a factor 10^3. The LHCb experiment has the potential to further improve this search, exploring a region potentially affected by new physics, using the data already recorded during 2012, corresponding to 2.0 fb^{-1}, i.e. twice the integrated luminosity of the 2011 sample. The sensitivity is expected to be improved, even more than by the larger statistics, by the increase of the trigger efficiency. Indeed, thanks to the increased trigger bandwidth (from 2.5 to 5 kHz), it was possible to select di–muon candidates of any invariant mass at the hardware trigger level, removing the 1 GeV/c^2 threshold that was excluding the K^0_S region during the 2011 run.

The much larger statistics needed to push the sensitivity to the SM level could be obtained during the LHCb upgrade phase, currently planned for 2019 onward, aiming at collecting 50 to 100 fb^{-1} of integrated luminosity.

References

[1] S. Gjesdal, *et al.*, Phys. Lett. B **44** (1973) 217.

[2] G. D'Ambrosio, G. Ecker, G. Isidori and H. Neufeld, hep-ph/9411439.

[3] J. Beringer *et al.* [Particle Data Group collaboration], Phys. Rev. D **86** (2012) 010001.

[4] G. Ecker and A. Pich, Nucl. Phys. B **366** (1991) 189.

[5] G. Isidori and R. Unterdorfer, JHEP **0401** (2004) 009 [hep-ph/0311084].

[6] A. A. Alves, Jr. *et al.* [LHCb collaboration], JINST **3** (2008) S08005.

[7] F. Archilli, W. Baldini, G. Bencivenni, N. Bondar, W. Bonivento, S. Cadeddu, P. Campana and A. Cardini *et al.*, arXiv:1306.0249 [physics.ins-det].

[8] X. Cid Vidal, CERN-THESIS-2012-154.

[9] A. L. Read, J. Phys. G **28** (2002) 2693.

[10] R. Aaij *et al.* [LHCb collaboration], JHEP **1301** (2013) 090 [arXiv:1209.4029 [hep-ex]].

PoS(KAON13)020